

## Exciton-carrier scattering in gallium selenide

Vito Capozzi

*Dipartimento di Fisica, Università di Bari, via Amendola 173, I-70126 Bari, Italy*

Lorenzo Pavesi

*Dipartimento di Fisica, Università di Trento, I-38050 Povo, Italy*

Jean Louis Staehli

*Institut de Physique Appliquée, Ecole Polytechnique Fédérale, PH-Ecublens, CH-1015 Lausanne, Switzerland*

(Received 17 December 1991)

Detailed investigation of the luminescence features due to the recombination of the exciton-free-carrier process in GaSe is presented. This process shows a well-resolved luminescence line and it is an efficient recombination process in this semiconductor, even at low temperatures. We report accurate photoluminescence spectra measured at 2 K as a function of the excitation intensity, of the excitation energy, and of the lattice temperature from 2 to 200 K. To discriminate between the different kinds of free carriers participating in exciton-carrier scattering in GaSe, we have computed the temperature dependence of the scattering probability of the direct excitons with different carriers: direct electrons, indirect electrons, and holes; we have found that the most probable exciton-carrier scattering process is that involving the coexistence of direct electron and hole collisions. Line shape of the exciton-carrier scattering as a function of the carrier temperature has been calculated and fitted to the experimental luminescence spectra from 2 to 200 K and a very good agreement is found. From the absorption spectra of GaSe, we obtained a direct estimate of the excitonic polarizability.

### I. INTRODUCTION

In photoexcited semiconductors, the luminescence spectra depend on the electron-hole (eh) pair density ( $n_t$ ).<sup>1</sup> For low eh pair density ( $n_t \ll n_M$ , where  $n_M$  is the Mott density), the excitonic recombinations dominate the spectra. At high eh pair density ( $n_t > n_M$ ), the formation of an eh plasma produces characteristic recombination bands. For intermediate eh pair density ( $n_t < n_M$ ), different features can be observed at energies lower than the absorption edge. In this region, the interaction between excitons ( $x$ ), electrons ( $e$ ), and holes ( $h$ ) become important. Consequently, inelastic scattering processes can open different radiative recombination paths. Luminescence from exciton-exciton ( $x-x$ ) and exciton-free-carrier ( $x-c$ ) scattering processes have been observed in many three-dimensional (3D) semiconductor compounds.<sup>1</sup>

In the last few years, the study of the  $x-c$  scattering has aroused new interest in 2D semiconductors as III-V quantum wells.<sup>2</sup> In particular, in 2D systems the  $x-c$  interaction is much more stronger than in 3D materials; this is a consequence of the considerably weaker screening of the Coulomb interaction in 2D compared with 3D.<sup>3</sup> Further, at present there is a debate on the importance of the  $x-c$  scattering process in quantum wells in achieving the relaxation of the photoexcited carriers.<sup>4</sup>

In GaSe, luminescence due to excitonic scattering has been already observed.<sup>5-9</sup> In particular, at low temperature, an emission line ( $XC$ ) at about 4 meV below the recombination of the direct exciton was attributed to the inelastic  $x-c$  scattering.<sup>5-9</sup> There are several open problems connected with this luminescence line.

(i) Supplementary detailed experimental data to support the interpretation of the  $XC$  line. In the literature, some authors have proposed the excitonic molecule as the origin for this line.<sup>10</sup>

(ii) Comparison with the experimental data about the  $x-c$  scattering in the II-VI or III-V semiconductors shows that in GaSe the  $x-c$  recombination process is a particular one. In fact, the  $XC$  luminescence is a relatively strong and narrow line and it is observed even at low lattice temperatures ( $T_L$ ).

(iii) Which kind of  $x-c$  scattering process occurs to explain this line is not clear yet. In fact, in GaSe the indirect conduction-band minimum at  $M$  point of the Brillouin zone is only 25 meV lower than the direct one at  $\Gamma$  (Fig. 1). Experimentally, it was found that optical excitation populates both minima.<sup>9,11</sup> Thus, at eh densities lower than the  $n_M$ , exciton-free-carrier recombinations will involve both conduction-band minima. In principle, any direct or indirect carrier populating the band extrema at  $\Gamma$  or  $M$  can interact with an exciton to originate the  $XC$  emission line.<sup>5,12</sup>

In this paper, we try to settle these questions through a detailed investigation of photoluminescence of GaSe at intermediate excitation intensities ( $J$ ) at which  $x-c$  scattering processes are efficient. We present photoluminescence (PL) spectra, measured at 2 K as a function of  $J$ , of the excitation energy and of the lattice temperatures from 2 to 200 K. We apply the theory of Hönerlage, Klingshirn, and Grun<sup>13</sup> to calculate the scattering probability of the different  $x-c$  processes as a function of the carrier temperature ( $T$ ) and to compute the associated line shape of the luminescence. We com-

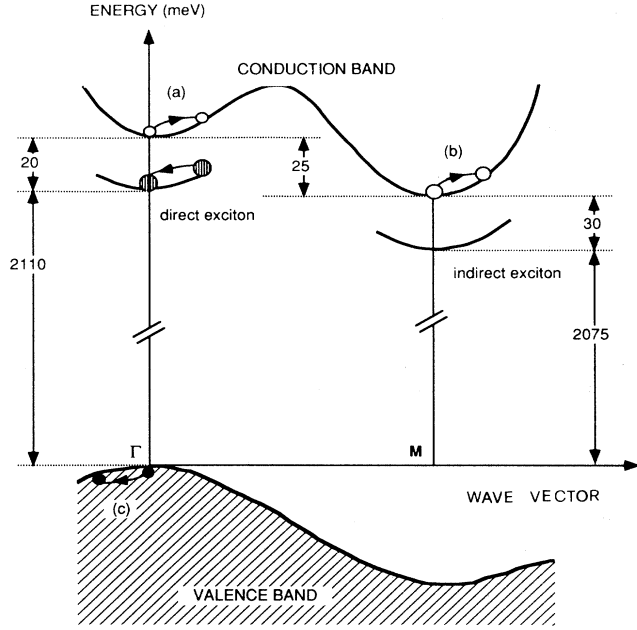


FIG. 1. Simplified sketch of the highest valence band and lowest conduction band of GaSe. The excitonic energies and the width of the direct gap are taken from Refs. 11, 20, and 23. Some excitonic-carrier scattering processes are also indicated and discussed in details in the text.

pare the theoretical results with the experimental spectra in the range of temperatures from 2 to 200 K. Preliminary results of this work were reported in Ref. 12.

## II. THEORY

### A. Different recombination processes

An exciton having a center-of-mass momentum  $\mathbf{K}_i$  different from zero can recombine radiatively only while it is interacting with another particle or with the crystal lattice. In addition to the *direct* radiative recombination of electrons, one distinguishes mainly recombinations assisted by optical phonons, by excitons, or by free carriers. Due to the conservation of energy and momentum during these recombination processes, the related luminescence lines are shifted to lower (and sometimes also to higher) energies.

As the *XC* line is observed very near to the spectral position of the direct exciton recombination, we study only *x-c* scattering that involves a direct exciton as the final excitonic state. We consider the following *x-c* scattering processes (Fig. 1):

$$(a) \quad x^\Gamma(\mathbf{K}_i) + e^\Gamma(\mathbf{k}_i) \rightarrow \hbar\omega + e^\Gamma(\mathbf{K}_i + \mathbf{k}_i),$$

$$(b) \quad x^\Gamma(\mathbf{K}_i) + e^M(\mathbf{k}_i) \rightarrow \hbar\omega + e^M(\mathbf{K}_i + \mathbf{k}_i),$$

$$(c) \quad x^\Gamma(\mathbf{K}_i) + h(\mathbf{k}_i) \rightarrow \hbar\omega + h(\mathbf{K}_i + \mathbf{k}_i),$$

$$(d) \quad x^M(\mathbf{K}_i) + e^\Gamma(\mathbf{k}_i) \rightarrow \hbar\omega + e^M(\mathbf{K}_i + \mathbf{k}_i),$$

where  $x^\sigma(\mathbf{K}_i)$  represents a direct ( $\sigma = \Gamma$ ) or indirect

( $\sigma = M$ ) exciton having the center-of-mass momentum  $\mathbf{K}_i \neq 0$ ,  $c^\sigma(\mathbf{k})$  is a free carrier ( $c = e$ ) or ( $c = h$ ) with wave vector  $\mathbf{k}_i$ , and  $\hbar\omega$  is the energy of the emitted photon.

We remark that the *x-c* scattering process (d) cannot explain the *XC* recombination. In fact, in this case, due to the energy conservation in the scattering, the energy of the emitted photon should be at least 10 meV lower than the energy of the direct exciton line (see the difference in the excitonic binding energy for the direct and indirect exciton given in Table I). Thus, to discuss the *XC* line we consider only the (a), (b), and (c) processes which concern only direct excitons in the initial state.

### B. Exciton-carrier line shape

The theoretical description of the *x-c* recombination process is usually based on a second-order perturbation picture. We use the formulation proposed by Hönerlage, Klingshirn, and Grun<sup>13</sup> which accounts for polaritonic effects, the momentum dependence of scattering matrix elements, and the thermal distribution of the excitons; it is very similar to the formulations proposed by Benoît à la Guillaume, Debever, and Salvan<sup>14</sup> or by Haug and Schmitt-Rink.<sup>15</sup>

In second-order perturbation theory and in the polariton formalism, the *x-c* recombination decomposes into two steps.<sup>13</sup> First, an exciton with a translational mass  $M_x$  scatters to a state with zero wave vector by interaction with a free carrier of effective mass  $m_c$ . Second, the exciton recombines (i.e., the polariton escapes from the crystal as a photon):

$$x(\mathbf{K}_i) + c(\mathbf{k}_i) \rightarrow x(\approx 0) + c(\mathbf{K}_i + \mathbf{k}_i) \rightarrow \hbar\omega + c(\mathbf{K}_i + \mathbf{k}_i). \quad (2.1a)$$

The energy conservation of the *x-c* process gives

$$E_0 + \frac{\hbar^2 \mathbf{K}_i^2}{2M_x} + E_g + \frac{\hbar^2 \mathbf{k}_i^2}{2m_c} = \hbar\omega + E_g + \frac{\hbar^2 (\mathbf{k}_i + \mathbf{K}_i)^2}{2m_c}, \quad (2.1b)$$

where  $E_0$  is the exciton energy at  $\mathbf{K} = 0$  and  $E_g$  is the energy gap. From Eq. (2.1b), one expects that the energy of the emitted photon is lower than  $E_0$ . Moreover, since the kinetic energy of *x* and *c* particles are thermally distributed, we also expect that the lineshape of the *x-c* recombination will depend on the carrier temperature.

TABLE I. The parameters of GaSe used in the calculations. Following Ref. 30, we accounted for the axiality of the crystal (Ref. 20) also in the effective masses (Ref. 29).

	Direct minimum	Indirect minimum
Exciton binding energy	20 meV	30 meV
Exciton translational mass	$0.44m_0$	$0.86m_0$
Exciton reduced mass	$0.10m_0$	$0.18m_0$
Electron mass	$0.17m_0$	$0.59m_0$
Hole mass	$0.27m_0$	

The luminescence intensity  $L(\hbar\omega)$  as given by Hönerlage, Klingshirn, and Grun<sup>13</sup> is proportional to the product

$$L(\hbar\omega) \propto P(\hbar\omega)F(\hbar\omega), \quad (2.2)$$

where  $P(\hbar\omega)$  is the probability that an exciton reaches a state of momentum  $\hbar\mathbf{K}=0$  through an  $x$ - $c$  scattering process (first step), and  $F(\hbar\omega)$  is the probability that the polariton leaves the crystal as a photon (second step). In particular, the expression for  $P(\hbar\omega)$  is given by

$$P(\hbar\omega) = 4\pi^3 \sum_c \frac{(m_c)^2}{\hbar^4 \beta} n_x n_c \Lambda_x^3 \Lambda_c^3 \int_0^\infty d\mathbf{K} \mathbf{K} |T_{fi}|^2 \exp \left\{ -\beta \left[ \frac{\hbar^2 K^2}{2M_x} + \frac{\hbar^2 b^2(\hbar\omega)}{2m_c} \right] \right\}, \quad (2.3)$$

with

$$\Lambda_c \equiv \left[ \frac{2\pi\hbar^2}{k_B T m_c} \right]^{1/2},$$

$$\Lambda_x \equiv \left[ \frac{2\pi\hbar^2}{k_B T M_x} \right]^{1/2},$$

and

$$b^2(\hbar\omega) \equiv \frac{(m_c)^2}{\hbar^4 K^2} \left[ \frac{\hbar^2 K^2}{2M_x} - \frac{\hbar^2 K^2}{2m_c} + \hbar(\omega_0 - \omega) \right]^2.$$

The sum  $\sum_c$  runs over the contributions of  $\Gamma$  electrons,  $M$  electrons, and holes to inelastic  $x$ - $c$  scattering,  $\beta \equiv 1/k_B T$ ,  $n_x$  and  $n_c$  are the densities of direct excitons and the free carriers,  $\hbar\omega_0 = E_0$ . The matrix element  $T_{fi}$  is defined through<sup>13</sup>

$$T_{fi} \delta(\mathbf{k}_i - \mathbf{k}_f + \mathbf{K}_i) \equiv \langle f | V | i \rangle, \quad (2.4)$$

where  $\mathbf{k}_f$  is the wave vector of the final state of the carrier.  $V$  is the scattering potential between the free carriers and the components of the exciton. Direct and exchange scattering takes place via the Coulomb interaction, statically screened by the free carriers. The screening constant appearing in  $V$  is a function of  $n_c$ .<sup>13</sup>  $T_{fi}$  is separable in a sum over the contributions due to the direct interaction between  $x$  and  $c$  ( $T^d$ ) and the contributions due to the exchange scattering between two homopolar particles ( $T^x$ ):

$$|T_{fi}|^2 = \sum_{v, v'} \left| T^d \delta_{v_1 v_1'} \delta_{v_2 v_2'} - T^x \delta_{v_1 v_2'} \delta_{v_2 v_1'} \right|^2. \quad (2.5)$$

where  $\sum_{v, v'}$  is over the different spin configurations of the initial and final states.

To apply Eq. (2.5) to GaSe we should consider the symmetry of this semiconductor. Due to its layered structure, the samples are usually thin plates with the  $c$  axis normal to the platelet plane. Thus, the luminescence is usually observed with light propagating in the  $c$  direction. The symmetry of GaSe is essentially determined by the space group  $D_{3h}^1$  of a single layer, because the electron densities are highest within the layers and because the interlayer interaction is small.<sup>16</sup> The radiative interband transitions at the  $\Gamma$  point of the Brillouin zone take place between conduction- and valence-band states belonging to the representations  $\Gamma_8$  and  $\Gamma_7$  of the double group  $\bar{D}_{3h}^1$ . Hence, for light propagating in the direction of the  $c$  axis, radiative  $\Gamma$ - $\Gamma$  transitions are only partially allowed through spin-orbit coupling. Furthermore, only

triplet  $s$  excitons participate in optical transitions.<sup>16</sup> Considering all the possible spin configurations for direct and exchange scattering, in the same way as was done in Ref. 13, Eq. (2.5) reduces to

$$|T_{fi}|^2 = |T^d|^2 + |T^x|^2 + |T^d - T^x|^2 \quad (2.6)$$

for  $x$ - $e^\Gamma$  and  $x$ - $h$  scattering. For exciton-indirect-electron scattering the exchange term is zero due to the fact that no exchange interaction is possible between the direct electron (which forms the exciton) and the indirect electron. Thus,

$$|T_{fi}|^2 = 2|T^d|^2. \quad (2.7)$$

In our formalism  $P(\hbar\omega)$  is independent of the exciton polarizability ( $\gamma$ ), while  $F(\hbar\omega)$  reflects the polariton dispersion in the direction of observation; if we neglect reabsorption and surface effects,  $F(\hbar\omega)$  is given by the photon part of the polariton final wave function:<sup>13,17</sup>

$$F(\hbar\omega) = \frac{[(c|\mathbf{Q}|/\omega_0) + (\omega/\omega_0)^2]}{4c|\mathbf{Q}|\omega/\omega_0^2} \times \frac{(1 - \omega^2/\omega_0^2)^2}{(1 - \omega^2/\omega_0^2)^2 + (4\pi\gamma/\varepsilon_0\omega_0)}, \quad (2.8)$$

where  $\varepsilon_0$  is the static dielectric constant and  $C|\mathbf{Q}|$  is given by the polariton dispersion

$$\frac{c^2 \mathbf{Q}^2}{\omega^2} = 1 + \frac{4\pi\gamma/(\varepsilon_0\omega_0)}{1 - \omega^2/\omega_0^2}. \quad (2.9)$$

The quantity  $2\pi\gamma/\varepsilon_0$  is approximated by the longitudinal transverse split  $\Delta\omega_{LT}$  of the polariton.<sup>17</sup>

To obtain  $\Delta\omega_{LT}$  we use the fact that the oscillator strength of the excitonic transition per unit volume,  $f/\Omega_0$ , is given by<sup>18</sup>

$$\int_{\text{exciton line}} \alpha(\omega) d\omega = \frac{2\pi^2 q^2 \hbar}{m v n} \frac{f}{\Omega_0}, \quad (2.10)$$

where  $\alpha$  is the absorption coefficient,  $q$  is the electronic charge,  $v$  is the light speed in vacuum, and  $n$  is the real part of the refraction index of the crystal.

Using the Lyddane-Sachs-Teller relation<sup>19</sup>

$$\varepsilon_0 = \varepsilon_\infty \frac{\omega_{LO}^2}{\omega_{TO}^2} \equiv \varepsilon_\infty \frac{(\omega_{TO} + \Delta\omega_{LT})^2}{\omega_{TO}^2} \equiv \varepsilon_\infty \left[ 1 + \frac{2\Delta\omega_{LT}}{\omega_{TO}} \right], \quad (2.11)$$

solving for  $\Delta\omega_{LT}$ , and using the dielectric function of a

classical oscillator, we obtain

$$\Delta\omega_{LT} = \frac{2\pi q^2 \hbar}{m\omega_0 \epsilon_\infty} \frac{f}{\Omega_0} = \frac{c}{\pi\omega_0 \sqrt{\epsilon_\infty}} \int_{\text{exciton line}} \alpha(\omega) d\omega. \quad (2.12)$$

Using the results of LeToullec *et al.*<sup>20</sup> for  $\alpha$  and  $\epsilon_\infty = 7.44$  (Ref. 20), we have

$$\hbar\Delta\omega_{LT} = 4.3 \times 10^{-5} \text{ eV}, \quad (2.13)$$

which is a direct estimate of the excitonic polarizability in GaSe. Note that no experimental data exist in the literature.

### C. Mass action law and exciton-carrier scattering probabilities

Since the samples we used were nominally undoped, we assume that the hole density is equal to the electron density. Hence, we write  $n_i = n^\Gamma + n^M$ , where  $n_i$  is the total photoexcited pair density and  $n^\Gamma$  or  $n^M$  is the pair density in which the electron belongs to the  $\Gamma$  minimum or  $M$  minimum of the conduction band. We assume intravalley equilibrium, i.e., each band extremum has its own chemical potential, but all carriers have the same temperature  $T$ . The densities of excitons (bound eh pairs,  $n_x^\sigma$ ) and dissociated eh pairs ( $n_c^\sigma$ ) are related by a mass action law,<sup>21</sup>

$$n^\sigma = n_c^\sigma + n_x^\sigma, \quad (2.14)$$

$$n_x^\sigma = \frac{1}{2} (n_c^\sigma)^2 \left[ \frac{2\pi\hbar^2}{k_B T \mu_x^\sigma} \right]^{3/2} e^{-\beta E_b^\sigma}, \quad (2.15)$$

where the excited  $x$  states have been neglected;  $\sigma$  denotes  $\Gamma$  or  $M$ ,  $\mu_x^\sigma$  is the exciton reduced mass, and  $E_b^\sigma$  the exciton binding energy. The free hole density is  $n_h = n_e^\Gamma + n_e^M$ . Due to the fact that the direct exciton binding energy is 20 meV and the indirect exciton binding energy is 30 meV (Table I), the density of free carriers in the  $M$  minimum is always smaller than the free-carrier density in the direct minimum. We do not assume intervalley equilibrium; the ratio  $n^\Gamma/n^M$  is a free parameter in our calculations.

To determine which exciton-carrier recombination process can explain the line  $XC$ , we computed in Fig. 2, as a function of  $T$  and for a fixed total eh pair density, the maximum of the recombination probability of  $x$ - $c$  scattering process [Eq. (2.3)] for the following four collision processes: (a) direct exciton-direct electron ( $x-e^\Gamma$ ), (b) direct exciton-indirect electron ( $x-e^M$ ), (c) direct exciton-hole ( $xh$ ), and (d) direct exciton-direct electrons+holes ( $x-e^\Gamma+x-h$ ). We remark that the process  $x-e^M$  scattering can be neglected at all temperatures because it has a very low probability (about two order of magnitude) compared to that of the processes  $x-e^\Gamma$  and  $x-h$ , in spite of the higher electron mass (see Table I) and higher density of states at the  $M$  minimum of the conduction band. This is due to the fact that the larger contribution to  $P(\hbar\omega)$  comes from the strongly probable exchange scattering<sup>13</sup> which is absent for the  $x-e^M$  collision process. Moreover, the cross section of such a scattering is small because of the wave-vector dependence of the

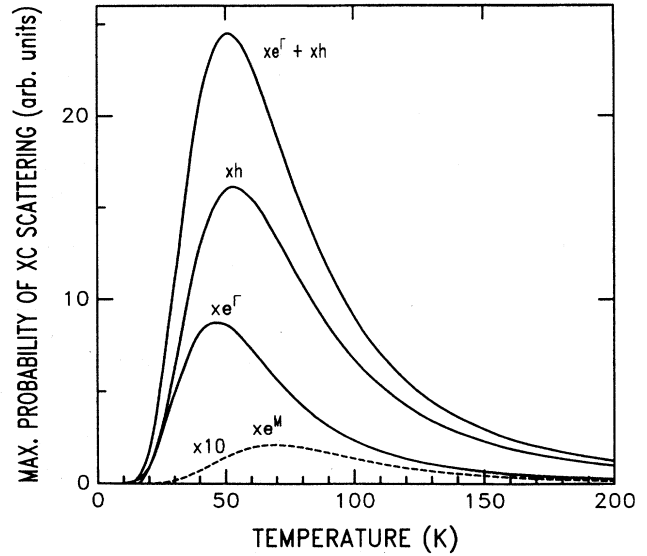


FIG. 2. Temperature dependence of the maximum probability  $P(\hbar\omega)F(\hbar\omega)$  [see Eqs. (2.3) and (2.8)] of exciton-carrier recombination in GaSe. It has been calculated for collision processes between excitons and direct electron ( $x-e^\Gamma$ ), exciton and indirect electrons ( $x-e^M$ ), excitons and holes ( $xh$ ), and excitons and both direct electrons + holes ( $x-e^\Gamma+xh$ ).

Coulomb interaction which decreases as  $(1/k_i)^2$ . In addition, the density of the indirect free carrier is smaller than that of the  $\Gamma$  electrons. On the other hand, the processes  $x-e^\Gamma$  and  $x-h$  have comparable probabilities in GaSe, particularly at low temperatures (below 25 K). This suggests that the emission  $XC$  is indeed a superposition of  $x-e^\Gamma$  and  $x-h$  recombination processes. In the following, we take this assumption to fit the  $XC$  line shape.

### III. EXPERIMENTAL TECHNIQUES

The GaSe crystals investigated were grown by the transport reaction method. Samples were selected on the basis of their excitonic transmission spectra, measured at a bath temperature of 2 K. The line width of the  $n=1$  excitonic line ranged between 2 and 5 meV. In some samples, the  $n=3$  exciton peak can be observed. The thickness of the crystal platelets was determined optically from the interference fringes in the transmission spectra, performed parallel to the  $c$  axis; it varied between 5 and 15  $\mu\text{m}$ . The crystals were immersed in superfluid He, optically excited by the frequency-doubled emission at 532 nm of a YAG:Nd laser (where YAG denotes yttrium aluminum garnet). The excitation pulses had a duration of about 90 ns and a repetition rate of 1 KHz. For the excitation PL spectra (PLE), the samples were excited by means of a dye laser (Rhodamine 6G pumped by line 532 nm of the YAG:Nd laser) whose pulses had a duration of 60 ns and a repetition rate of 75 Hz. The dye laser was used as a variable monochromatic source, thus allowing resonant excitation of the excitonic levels and of the conduction-band free states.

The diameter of the illuminated spot on the samples

measured about  $70 \mu\text{m}$ . The emitted light was collected from the front face of the sample in a direction forming an angle of  $\pi/4$  with respect to the  $c$  axis. A pin hole was placed in the image plane of the collecting lens so that only light coming from the excited volume was detected. The luminescence was analyzed by a double spectrometer (linear dispersion  $5 \text{ \AA}/\text{mm}$ ) and detected by a photomultiplier tube cooled at  $253 \text{ K}$ . The PL spectra were measured using a boxcar technique and recorded by means of a multichannel system. The intensity  $J$  absorbed by the sample was varied by a set of calibrated neutral-density filters between  $1 \text{ kW cm}^{-2}$  and  $0.3 \text{ MW cm}^{-2}$ . The absorption coefficient of GaSe at  $532 \text{ nm}$  is about  $10^3 \text{ cm}^{-1}$ .<sup>20</sup> Assuming a carrier life time of  $0.1 \text{ ns}$ ,<sup>22</sup> the total  $e-h$  pair density created at the surface of the sample, ranged from  $3 \times 10^{14} \text{ cm}^{-3}$  to  $8 \times 10^{16} \text{ cm}^{-3}$ . The Mott transition of direct exciton is expected to occur for  $e-h$  pair densities of about  $10^{17} \text{ cm}^{-3}$ .<sup>21</sup>

#### IV. RESULTS AND DISCUSSION

Figure 3 shows PL spectra of a sample of GaSe measured at a temperature of  $2 \text{ K}$  and at different excitation intensities. The emission line  $X$  at  $587.5 \text{ nm}$  is due to the well-known recombination of the fundamental direct free

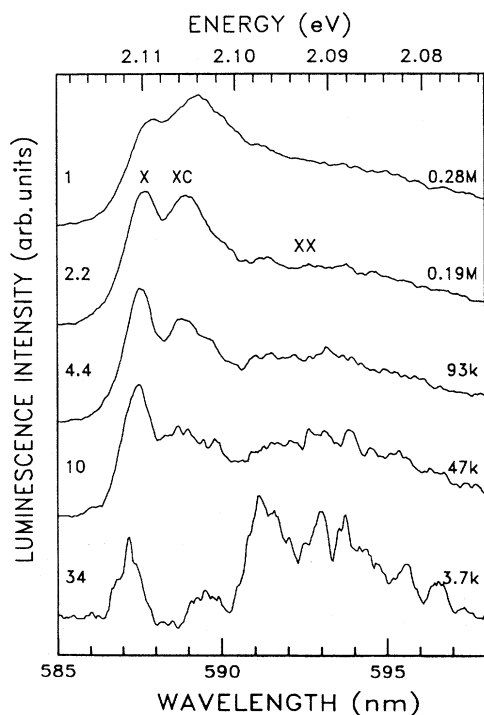


FIG. 3. Luminescence spectra of a transport-grown sample of GaSe (about  $10 \mu\text{m}$  thick) immersed in a superfluid helium bath at a temperature of  $2 \text{ K}$  and photoexcited by a frequency-doubled YAG:Nd laser at  $532 \text{ nm}$ . For each spectrum the different pump intensities in  $\text{W cm}^{-2}$  are indicated (right-hand side), as well as the relative scale factors for the luminescence intensities (left-hand side). The labels have the following meaning:  $X$ , direct free exciton;  $XC$ , exciton-carrier scattering;  $XX$ , exciton-exciton scattering. Spectral resolution is  $0.2 \text{ nm}$ .

exciton.<sup>23</sup> This line is well resolved for laser intensities lower than about  $0.2 \text{ MW cm}^{-2}$ . At lower energies, different structures due to the various scattering processes occurring in a dense exciton gas appear.<sup>1,9</sup> In particular, the  $XC$  emission at  $589 \text{ nm}$  is attributed to excitonic recombination assisted by an exciton-carrier scattering process.<sup>5-9</sup>

We discuss now several experimental results which support this assignment. The integrated emission intensity of the  $XC$  line increases versus  $J$ , more rapidly than that of the  $X$  line. In fact, for  $J$  lower than  $0.3 \text{ MW cm}^{-2}$ , we found (see Fig. 4) that the integrated luminescence intensities ( $L_{xc}$ ) of the line  $XC$  is related to the intensity of the exciton line ( $L_x$ ) by

$$L_{xc}(J) \sim L_x(J)^{3/2}. \quad (4.1)$$

Thus,  $L_{XC}$  is proportional to  $(n_x)^{3/2}$ , in agreement with theoretical predictions for an  $x-c$  scattering process<sup>14</sup> and with previous experimental results for GaSe (Refs. 5 and 9) and ZnO.<sup>24</sup> The  $X$  and  $XC$  lines become wider and gradually shift to longer wavelengths when the carrier density increases (see also Ref. 21).

The smallness of the polarizability in GaSe ( $\hbar\Delta\omega_{LT} \approx 4.3 \times 10^{-5} \text{ eV}$ ), for light propagating in the  $c$  direction explains the narrowness of the  $x-c$  recombination line (Fig. 3). On the contrary, in the II-VI compounds, the splitting  $\hbar\Delta\omega_{LT}$  is larger than  $1 \text{ meV}$ .<sup>1</sup> In these compounds the luminescence lines due to the  $x-c$  scattering processes are indeed larger than in GaSe and not resolved from the free-exciton line even at low temperatures.

At the lowest excitation intensities ( $J \approx 3.7 \text{ kW cm}^{-2}$ ) a weak structure appears at about  $590 \text{ nm}$ . This line was attributed to the recombination of a direct exciton bound

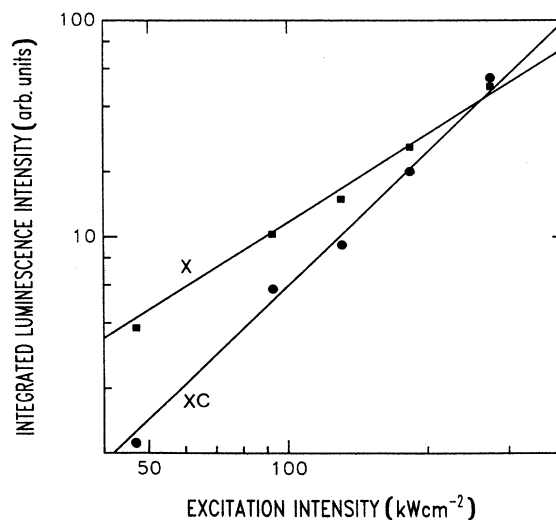


FIG. 4. Logarithmic plots of the integrated luminescence intensity ( $L$ ) of the direct free exciton line ( $X$ ) and of the exciton-carrier recombination ( $XC$ ) versus pump intensity ( $J$ ). Continuous lines are least-square fits of the experimental intensities (dots) to the single power law  $L \sim J^s$ . The exponent  $s$  is  $2.0$  for the  $XC$  line and  $1.3$  for the  $X$  luminescence.

to an impurity donor level<sup>25</sup> and it saturates at  $J$  of about  $50 \text{ kW cm}^{-2}$ . The broad band ( $XX$ ) that appears at wavelengths longer than  $590 \text{ nm}$  is structured at the lowest laser intensities. This band is due to the overlapping emission coming from direct as well as indirect exciton-exciton scattering processes, whose recombination energies are reported in Ref. 9.

For  $J$  larger than  $0.2 \text{ MW cm}^{-2}$  the  $XC$  emission gradually dominates the PL spectra. Moreover, the  $X$  line broadens and appears as a shoulder on the high-energy side of the  $XC$  emission. In this range of  $J$ , the spectral position of the  $X$  and  $XC$  lines are nearly independent of  $J$ . As  $J$  is further raised, when the complete ionization of the excitons occurs [Mott transition of direct excitons occurs for an  $eh$  pair density of about  $10^{17} \text{ cm}^{-3}$  (Ref. 21)] the  $XC$  line is replaced by a broad band due to the direct  $e-h$  plasma. Moreover, the intensity of the  $XX$  band decreases with respect to that of the lines  $X$  and  $XC$ , and it is replaced by the indirect  $e-h$  plasma which contains  $M$  electrons and  $\Gamma$  holes.<sup>11</sup>

Figure 5 shows PLE spectra of the emission  $XC$  detected at  $589 \text{ nm}$  for the same sample of Fig. 1, measured at  $T_L = 2 \text{ K}$  and for several excitation intensities. We ob-

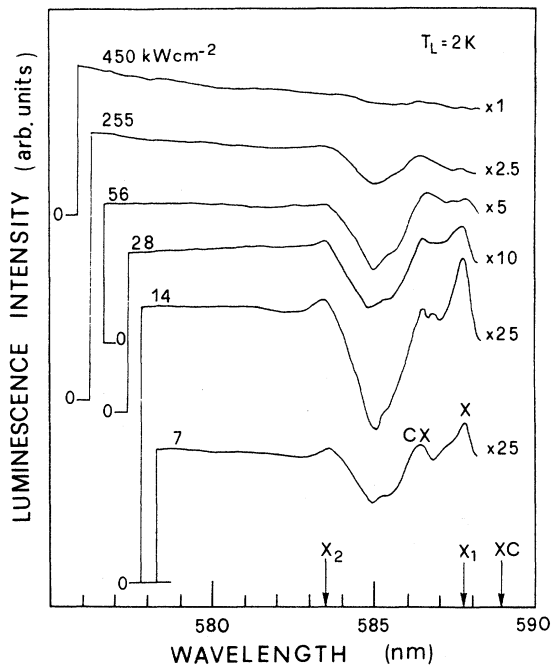


FIG. 5. Luminescence excitation spectra of the line  $XC$  at  $589 \text{ nm}$  of the same sample of GaSe as in Fig. 3, measured at the He-bath temperature of  $2 \text{ K}$  and photoexcited by a dye laser (rhodamine 6 G), pumped by a frequency-doubled YAG laser at  $75 \text{ Hz}$ . For each spectrum the different excitation intensities in  $\text{kW cm}^{-2}$  are indicated (left-hand side), as well as the relative scale factors of the luminescence intensities (right-hand side). The arrows indicate the spectral position of the two lowest direct excitonic levels ( $X_1$  and  $X_2$ ), as well as that of the  $XC$  emission. For the meaning of the  $CX$  structure, see the text. Light was collected from the front face of the crystal. Spectral resolution is of  $0.2 \text{ nm}$ .

serve that the intensity of the PLE spectra of this line increases resonantly with the lowest direct free-exciton states  $x_1$  at  $587.7 \text{ nm}$  and  $x_2$  at  $583.5 \text{ nm}$ . In other words, when the exciton levels are resonantly excited, there is a direct contribution from these states to the  $XC$  emission. The same occurs when the states of the conduction band are selectively excited. We observe that the photogenerated electrons in the conduction band contribute to the emission  $XC$  with an efficiency comparable to that of the excitonic states. When  $J$  increases, the exciton resonances broaden and become less and less resolved (as happens in the spectra of Fig. 3), tending progressively to disappear. For  $J$  higher than  $0.4 \text{ MW cm}^{-2}$ , the PLE spectra become flat; this is due to the lowering of the conduction band and to the consequent disappearing of the exciton states, indicating that the Mott transition of the direct excitons has occurred.<sup>21</sup>

At  $586.5 \text{ nm}$  there is another structure ( $CX$ ) which is about  $4 \text{ meV}$  from the  $X$  line. Its intensity increases versus  $J$  more rapidly than that of the  $X$  resonance and it is practically absent at low excitation intensities. This behavior is a further support to the interpretation of the  $XC$  line as being due to the  $x-c$  recombination process. In fact, we think that the reverse of the  $x-c$  scattering process is occurring. An exciton virtually absorbs a photon whose energy  $\hbar\omega$  is larger than that of the excitonic state at  $\mathbf{K}=0$ . The collision with an electron of energy  $\epsilon_i$  and wave vector  $\mathbf{k}_i$  permits the exciton to lose some energy and to gain a nonzero wave vector. At the same time, the electron scatters to a state having energy  $\epsilon_f$  and wave vector  $\mathbf{k}_f$ . The energy conservation implies that the photon involved in this process has an energy

$$\hbar\omega = E_0 + \epsilon_f - \epsilon_i, \quad (4.2)$$

which is larger than  $E_0$  of the amount  $(\epsilon_f - \epsilon_i) \approx 4 \text{ meV}$ . Indeed, the spectra position of the  $CX$  structure is symmetric to the line  $XC$  with respect to the excitonic emission line supporting our model.

Figure 6 shows a series of PL spectra measured at various temperatures and at a constant laser intensity of  $65 \text{ kW cm}^{-2}$  (corresponding to a total  $e-h$  pair density of about  $2 \times 10^{16} \text{ cm}^{-3}$ ). This figure gives further support to the interpretation of the  $XC$  line. In fact, the exciton-carrier scattering process becomes progressively more probable when the carrier temperature and thus their density  $n_c$  increases [see Eq. (2.3)]. On the other hand,  $n_x$  decreases as a function of  $T_L$  because of the thermal ionization of the excitons. Since the probability of the  $x-c$  scattering process is proportional to  $n_x n_c$ , we expect a temperature dependence of the  $XC$  intensity which at first increases and then decreases by raising the crystal temperature. This behavior is indeed observed in Fig. 6 and it is qualitatively in agreement with the theoretical prediction shown in Fig. 2.

For  $T_L$  below about  $40 \text{ K}$ , the two lines  $X$  and  $XC$  are resolved, depending on the excitation intensity, and their spectral position does not change. We note that at the lowest temperatures the energy difference between the  $X$  and  $XC$  lines should tend to zero since the free-carrier wave vector, which is proportional to the kinetic energy

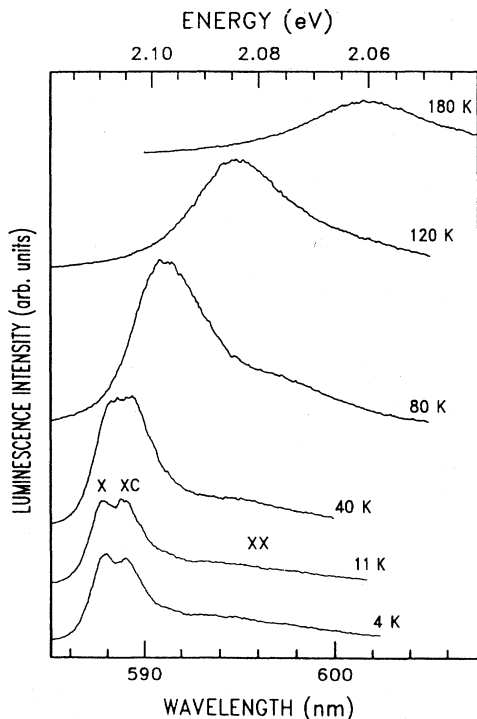


FIG. 6. Luminescence spectra of a transport-grown sample of GaSe (about  $5 \mu\text{m}$  thick), measured at different lattice temperatures. The sample was photoexcited by the frequency-doubled YAG:Nd laser at a pump intensity of  $65 \text{ kW cm}^{-2}$ , corresponding to a total  $e-h$  pair density of  $2 \times 10^{16} \text{ cm}^{-3}$ , calculated by assuming an  $e-h$  recombination time of  $0.1 \text{ ns}$  (Ref. 22) and an absorption coefficient of  $10^3 \text{ cm}^{-1}$  (Ref. 20). Spectral resolution is  $0.2 \text{ nm}$ . The labels have the same meaning as those in Fig. 3.

and hence to the electron-gas temperature, vanishes. This discrepancy between theoretical expectation and experimental data is explained below. For  $T_L$  higher than  $40 \text{ K}$ , the  $X$  and  $XC$  lines merge in a single band that shifts to lower energies because of the thermal reduction of the energy gap.

For completeness, we mention that the interpretation of the  $XC$  line as due to the radiative recombination of a phonon replica is not possible because an optical phonon of  $4 \text{ meV}$ , which should assist the transition, are not known in GaSe.<sup>26</sup> Moreover, the  $J$  dependence of the  $XC$  line should, in this case, be equal to that of the  $X$  line, because the probability of this process is proportional to  $n_x$ .

The line  $XC$  was attributed by some authors to the recombination of excitonic molecules.<sup>10</sup> This interpretation cannot be supported by the presence of this line in PL spectra measured at high temperatures (up to  $300 \text{ K}$ ). In fact, the biexciton binding energy in GaSe is about  $2 \text{ meV}$  (Ref. 24) and, thus, the excitonic molecule would thermally dissociate even at low temperatures. On the contrary, we observed an increase of the  $XC$  line intensity when  $T$  grows up to  $80 \text{ K}$  (Fig. 6). Moreover, the  $J$  dependence of the luminescence intensity of the  $XC$  emission is also in disagreement with this interpretation. In

fact, in such a case its integrated intensity should increase quadratically versus the emission intensity of the  $X$  line, because the probability of formation of biexcitons is proportional to  $n_x^2$ .<sup>14</sup> On the contrary, we found the dependence shown in Eq. (4.1), which is typical of an  $x-c$  recombination process.<sup>9,14</sup> Furthermore, in two beam experiments, no induced absorption structure (*giant absorp-*

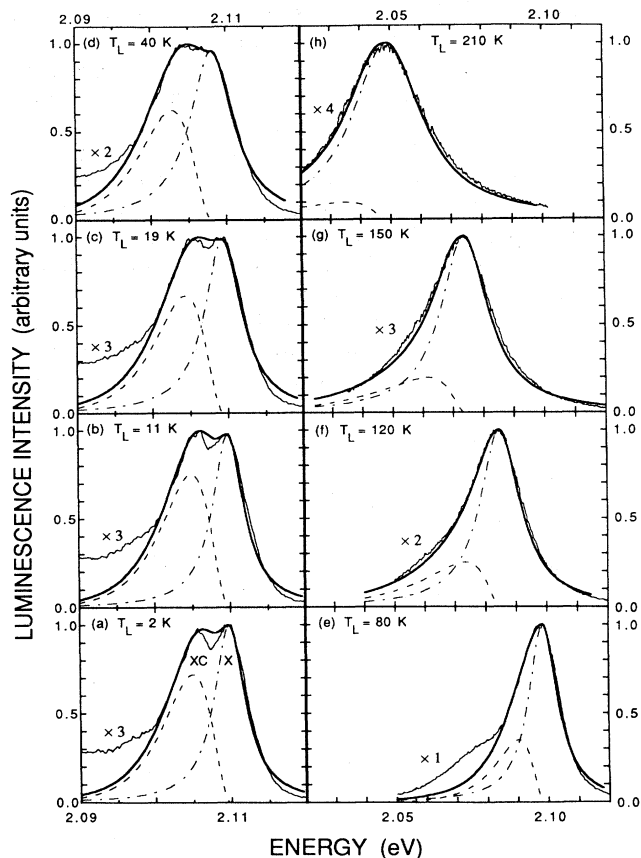


FIG. 7. Luminescence spectra (thin curve) of a sample of GaSe (the same as in Fig. 6) measured at various lattice temperatures ( $T_L$ ) under the same experimental conditions as described in the caption of Fig. 3. The sample was photoexcited by a laser intensity of  $65 \text{ kW cm}^{-2}$ , which corresponds to a total  $e-h$  pair density ( $n_t$ ) of  $2 \times 10^{16} \text{ cm}^{-3}$ . The thick curve is the calculated luminescence spectrum, which is the sum of the direct exciton line  $X$  (chain curve) and exciton-free carrier  $XC$  recombination (dashed curve). The calculated exciton line is a Lorentzian whose peak position and line width, deduced from experimental spectra, are reported in Table II. The line shape of the exciton-free-carrier (direct electrons and holes) recombination were calculated following Ref. 13 and Eq. (2.2) and using the crystal parameters of the Table I. The remaining common input parameters to fit the  $XC$  line shape are the exciton-polariton factor  $=4.3 \times 10^{-5} \text{ eV}$  (see Sec. II B) and the ratio  $R$  of direct to indirect electron density  $n^\Gamma/n^M=2$  (Ref. 11). The free parameters particular for each spectrum are the carrier temperature  $T$  and the relative intensity ( $F$ ) of the  $XC$  line with respect to that of the exciton (see Table II). The relative sensitivity factors for the luminescence intensity are indicated on the left-hand side of each spectrum. Spectral resolution is  $0.2 \text{ nm}$ .

tion) was observed for  $J$  lower than that of the Mott transition, apart from the usual excitonic absorption.<sup>28</sup>

To calculate the line shape for the exciton-carrier scattering process [Eq. (2.2)], we used the crystal parameters of Table I. Here, the values of carrier masses, obtained from the tensor components of the effective density-of-states masses of GaSe,<sup>29</sup> have been averaged (*dielectric average*), as was proposed in Ref. 30, to include the dielectric anisotropy. This average is appropriate for anisotropic crystals. The excitonic Rydberg and Bohr radius have been also calculated using the averaged dielectric masses of Table I, the components of static dielectric constant,<sup>20</sup> and the anisotropy factor of GaSe.<sup>20</sup> The remaining input parameters to fit the luminescence line shape of the  $x$ - $c$  scattering process are the following: (a) the total  $e$ - $h$  pair density  $n_t$ ; (b) the density ratio  $R$  between direct and indirect electrons; (c) the carrier temperature  $T$ .

We found that  $n_t$  influences the intensity and only weakly the line shapes of the  $x$ - $c$  recombination process (this is true for a nondegenerate limit). One has to increase  $n_t$  by several orders of magnitude to shift this line and broaden its linewidth by a few percent. For  $n_t$  we used the values deduced from the experimental excitation intensity, obtained in the usual way from the absorption coefficient<sup>20</sup> and lifetime of the  $eh$  pairs.<sup>22</sup> The parameter  $R$  scarcely influences the linewidth and spectral position of the calculated  $x$ - $c$  emission, because the line shape of  $x$ - $e^\Gamma$  and  $x$ - $h$  processes are quite similar. We have taken  $R = 2$  using the results obtained in Ref. 11 for the direct and indirect electron densities in the corresponding minima of the conduction band, which we assume are not in thermal equilibrium.<sup>11,13</sup> The carrier temperature is the *free* parameter to fit the  $x$ - $c$  line shape. We remark that the  $x$ - $c$  line shape is very sensitive to the carrier temperature. By increasing  $T$ , even a few degrees, a noticeable broadening of the  $XC$  linewidth and a redshift of its maximum is observed.

In Fig. 7, we compare a series of PL spectra, measured at various  $T_L$  with the line shapes obtained from the coexistence of  $x$ - $e^\Gamma$  and  $x$ - $h$  scattering processes. A Lorentzian line shape (chain curve at higher energy) has also been included in the calculation to fit the excitonic

line. The energy of its maximum  $E_0$  and that of the linewidth are deduced from the experimental spectra (see Table II). The relative intensity of the  $x$ - $c$  line shape (dashed curve at lower energy), with respect to that of the exciton line, was introduced as parameter to sum the line shapes of the two features. The results of the fit (thick curve) are quite good if we consider the approximations introduced in the model.<sup>13</sup> We remark that the strong low-energy tail of the exciton Lorentzian line prevents (mainly at low temperatures) fitting of the experimental PL spectra between the two lines. Further, the low-energy tail cannot fit the experimental data because of the presence of the  $XX$  luminescence band, whose contribution is more important at low temperatures (below 100 K). In fact, by increasing the temperature, the probability of the  $x$ - $x$  scattering decreases because of the exciton ionization and thus the intensity of the  $XX$  emission bleaches.

From the fits of Fig. 7 we got carrier temperatures (see Table II) that are in agreement with the estimate obtained from the high-energy tail of the exciton line. At low crystal temperature, the  $T$  values obtained from the line-shape analysis [see spectra (a) and (b)] are higher than  $T_L$ . This is in agreement with the results of Ref. 9 and with the temperature deduced from the redshift of the  $X$  line as a function of the carrier density, measured at  $T_L = 2$  K.<sup>21</sup> This lack of thermalization between excited carriers and crystal lattice is due to two reasons: (i) the laser energy (2.33 eV) is much higher than the bottom of the GaSe conduction band (2.13 eV), (ii) the short exciton lifetime [about 0.1 ns (Ref. 22)] prevents an efficient thermalization between the excited carriers and crystal lattice. For temperatures higher than 20 K, the values of  $T$  obtained from the fit coincide with the lattice temperature because the phonon density as well as the probability of the phonon-carrier scattering increases with  $T_L$ ; this fact facilitates the thermal equilibrium between lattice and photoexcited particles.

We remark that the theory of Hönerlage, Klingshirn, and Grun<sup>13</sup> has been formulated for the nondegenerate case in which Maxwell-Boltzman distribution is a good approximation for bound and free  $eh$  pairs. Our PL spectra, for  $T = 20$  K and  $n_t = 2 \times 10^{16}$  cm<sup>-3</sup>, are still a good

TABLE II. Parameters obtained from the line-shape analysis of the luminescence spectra of Fig. 6.  $T_L$  is the crystal temperature,  $E_0$  is the experimental spectral position of the peak of the exciton line,  $T$  is the carrier temperature,  $F$  is the ratio of the intensity of the  $XC$  line relative to that of the  $X$  line,  $n_t$  is the total electron-hole pair density, and  $R$  is the density ratio of direct electrons to indirect ones.

Spectrum	$T_L$ (K)	$E_0$ (eV)	Exciton linewidth (meV)	$T$ (K)	$F$	$n_t$ (cm <sup>-3</sup> )	$R$
(a)	2	2.1098	5.0	18	0.72	$2 \times 10^{16}$	2.0
(b)	11	2.1098	5.0	18	0.77	$2 \times 10^{16}$	2.0
(c)	19	2.1094	6.0	19	0.68	$2 \times 10^{16}$	2.0
(d)	40	2.1081	7.0	40	0.55	$2 \times 10^{16}$	2.0
(e)	80	2.0985	11.5	80	0.35	$2 \times 10^{16}$	2.0
(f)	120	2.085	16.0	120	0.25	$2 \times 10^{16}$	2.0
(g)	150	2.074	19.0	150	0.20	$2 \times 10^{16}$	2.0
(h)	210	2.049	28.0	210	0.10	$2 \times 10^{16}$	2.0



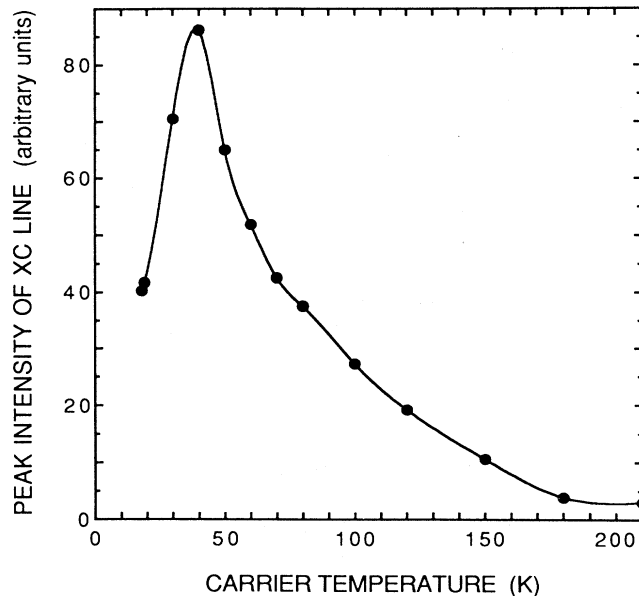


FIG. 8. Carrier-temperature dependence of the peak intensity of the line shape obtained from the exciton-free-carrier (direct electrons and holes) recombination that fits the experimental luminescence spectra of which a few are shown in Fig. 7. The continuous line is a guide for the eye.

approximation of a nondegenerate case. We remember that the Mott transition of direct excitons occurs at  $n_i \approx 1 \times 10^{17} \text{ cm}^{-3}$ .

Figure 8 shows the  $T$  dependence of the peak intensity of the emission line obtained from the  $x$ - $c$  (direct electrons and holes) recombinations which fit the experimental PL spectra of Fig. 7. This picture has a shape similar to the curve  $x-e^T + x-h$  of Fig. 2 and shows a maximum at about 40 K. This result is a further support to the  $x$ - $c$  scattering interpretation of the  $XC$  line and represents a good test of the model of Ref. 13, also at low crystal temperatures. The different peak position of the curves in Figs. 2 and 8 can be due to either the changes of the carrier lifetime, or the opening of further nonradiative recombination channels when  $T_L$  varies from 2 to 200 K.

## V. CONCLUSIONS

In GaSe there are several experimental evidences (e.g., the  $J$  dependence, the excitation spectra and the temperature evolution of the PL spectra) that support the interpretation of the  $XC$  emission line, at about 4 meV from the direct free-exciton recombination, as being due to the luminescence from an exciton-free-carrier scattering process. We applied the theory of Hönerlage, Klingshirn, and Grun<sup>13</sup> to calculate the scattering probabilities of the direct excitons with the different carriers (direct electrons, indirect electrons and holes) and we found that the most probable exciton-carrier scattering process is that involving the coexistence of direct electron and hole collisions. Another example of this simultaneous contribution was found for ZnSe.<sup>32</sup> Moreover, we have introduced a mass-action law between free and bound carriers in the two minima of the conduction band to calculate the line shape of the exciton-carrier scattering as a function of temperature. Experimental luminescence spectra from 2 to 200 K have been fitted and we found a very good agreement.

We have obtained the polariton factor of GaSe from the absorption spectra (see Sec. II B) and we found a value of  $4.3 \times 10^{-5}$  eV, which is much lower than those of the II-VI compounds [ $> 10^{-3}$  eV (Ref. 1)]. This is in agreement with the small polarizability of the III-VI semiconductors with respect to that of the II-VI materials. We believe that this work settles the issue of the interpretation of the  $XC$  luminescence line on the low-energy side of the excitonic recombination.

## ACKNOWLEDGMENTS

We are grateful to B. Hönerlage and L. C. Andreani for many helpful and stimulating discussions. We express our thanks to H. Berger and F. Levy for providing the fine GaSe samples. This work was in part supported by the "Consiglio Nazionale delle Ricerche" and by the "Fond National de la Recherche Scientifique". One of us (V.C.) wishes to thank, for their kind hospitality, the Institut de Physique Appliquée of the Ecole Polytechnique Fédérale de Lausanne, where the experiments were performed.

<sup>1</sup>See, e.g., C. Klingshirn and H. Haug, Phys. Rep. **70**, 315 (1981).

<sup>2</sup>R. Cingolani and K. Ploog, Adv. Phys. **40**, 535 (1991).

<sup>3</sup>A. Honold, L. Schultheis, J. Kuhl, and C. W. Tu, Phys. Rev. B **40**, 6442 (1989).

<sup>4</sup>T. Mishina and Y. Masumoto, Phys. Rev. B **44**, 5664 (1991).

<sup>5</sup>A. Mercier and J. P. Voitchovsky, Phys. Rev. B **11**, 2243 (1975).

<sup>6</sup>T. Ugumory, K. Masuda, and S. Namba, II Nuovo Cimento **38B**, 596 (1977).

<sup>7</sup>I. M. Catalano, A. Cingolani, M. Ferrara, and A. Minafra, Phys. Status Solidi B **68**, 341 (1975).

<sup>8</sup>N. Kuroda and Y. Nishina, J. Lumin. **12/13**, 623 (1976).

<sup>9</sup>V. Capozzi and J. L. Staehli, Phys. Rev. B **28**, 4461 (1983).

<sup>10</sup>M. S. Brodin, V. P. Kaperko, and M. G. Matsko, Fiz. Tekh.

Poluprovodn. **17**, 1568 (1983) [Sov. Phys. Semicond. **17**, 998 (1983)]; R. A. Taylor, S. E. Broomfield, J. F. Ryan, and F. Levy, in *Proceeding of the 18th International Conference on the Physics of Semiconductors*, edited by O. Enström (World Scientific, Singapore, 1987), p. 1811.

<sup>11</sup>J. L. Staehli and V. Capozzi, Helv. Phys. Acta **58**, 262 (1984).

<sup>12</sup>V. Capozzi, L. Pavesi, and J. L. Staehli, J. Lumin. **48**, 111 (1991).

<sup>13</sup>B. Hönerlage, C. Klingshirn, and J. B. Grun, Phys. Status Solidi B **78**, 599 (1976).

<sup>14</sup>C. Benoît à la Guillaume, J. M. Debever, and F. Salvan, Phys. Rev. **177**, 567 (1969).

<sup>15</sup>H. Huang and S. Schmitt-Rink, Prog. Quantum Electron. **9**, 3 (1984).

<sup>16</sup>E. Mooser and M. Schlüter, Nuovo Cimento **18B**, 164 (1973).

- <sup>17</sup>J. J. Hopfield, *Phys. Rev.* **182**, 945 (1969).
- <sup>18</sup>F. Bassani and M. Altarelli, *Handbook of Synchrotron Radiation*, edited by D. E. Eestman (North-Holland, Amsterdam, 1983), Vol. II, Chap. 7.
- <sup>19</sup>N. W. Ashcroft and N. D. Mermin, in *Solid State Physics* (Holt, Rinehart and Winston, London 1987), p. 548.
- <sup>20</sup>R. Le Toullec, N. Piccioli, M. Mejatty, and M. Balkansky, *Nuovo Cimento* **38B**, 159 (1977); R. Le Toullec, N. Piccioli, and J. C. Chervin, *Phys. Rev. B* **22**, 6162 (1980).
- <sup>21</sup>L. Pavesi, J. L. Staehli, and V. Capozzi, *Phys. Rev. B* **39**, 10982 (1989).
- <sup>22</sup>T. Kushida, F. Minami, Y. Oka, Y. Nazakaki, and Y. Tanake, *Il Nuovo Cimento* **39B**, 650 (1977); J. Collet (private communication).
- <sup>23</sup>A. Mercier, E. Mooser, and J. P. Voitchovsky, *Phys. Rev. B* **12**, 4307 (1975).
- <sup>24</sup>C. Klingshirn, *Phys. Status Solidi B* **71**, 547 (1975).
- <sup>25</sup>J. P. Voitchovsky and A. Mercier, *Il Nuovo Cimento* **22B**, 273 (1974).
- <sup>26</sup>S. Jandl, J. L. Brebner, and B. M. Powell, *Phys. Rev. B* **13**, 686 (1976).
- <sup>27</sup>O. Akimoto and Hamanura, *J. Phys. Soc. Jpn.* **33**, 1537 (1972).
- <sup>28</sup>J. L. Staehli and A. Frova, *Physica* **99B**, 299 (1980).
- <sup>29</sup>G. Ottaviani *et al.*, *Solid State Commun.* **14**, 933 (1974).
- <sup>30</sup>J. J. Hopfield and D. G. Thomas, *Phys. Rev.* **122**, 35 (1961).
- <sup>31</sup>V. Capozzi and M. Montagna, *J. Phys.* **46**, 191 (1985).
- <sup>32</sup>W. Maier and C. Klingshirn, *Solid State Commun.* **28**, 13 (1978).